Available online at www.sciencedirect.com
SCIENCE DIRECT®

Journal of the European Ceramic Society 24 (2004) 1987–1991
www.elsevier.com/locate/jeurceramsoc

Microstructure and mechanical properties of PZT fibres

X. Kornmann*, C. Huber

Polymers/Composites Laboratory, Swiss Federal Laboratories for Materials Testing and Research, CH-8600 Dübendorf, Switzerland

Received 27 February 2003; accepted 17 May 2003

Abstract

The single fibre test was used to determine the stress–strain behaviour and the strength distribution of three commercially available PZT-5A fibres with an approximate diameter of 250 μm. One of the fibres was manufactured via an extrusion process, whereas the others were produced via similar spinning processes. All the fibres presented a non-linear stress–strain behaviour, which is apparently linked to their piezoelectric nature. The Young's modulus of the fibres varied between 38 and 40 GPa. The strength distribution analysis (i.e. Weibull analysis) indicated large differences between the fibres with scale parameters varying between 49 and 68 MPa, and shape parameters situated between 4 and 12. These results were well correlated with the presence of defects in the fibres observed under a microscope. The fibres with the lowest scale and shape parameters, manufactured via a spinning process, contained large porosities and their diameter was varying along their length. In contrast, the two other fibres produced via different manufacturing processes (extrusion and spinning) presented better strength properties and a more homogeneous microstructure.

Keywords: Fibres; Mechanical properties; Microstructure-final; PZT; PZT fibres; Strength

1. Introduction

Piezoelectric fibre composites present many advantages over conventional piezoelectric materials because they combine low density and high flexibility with good electromechanical performances. Piezoelectric ceramic fibres made of lead zirconate titanate [PZT: Pb(Zr, Ti)O_3] are increasingly used to manufacture smart composites, which find their use in various types of applications. Rod composites (i.e. 1–3 composites) have been developed for use as ultrasonic transducers[1] and sonar in submarines. Active fibre composites (AFCs) (i.e. 1–2 composites) constituted of uniaxially aligned piezoelectric fibres sandwiched between interdigitated electrodes and embedded in a polymer matrix have been recently developed in the Active Materials and Structure Laboratory at the Massachusetts Institute of Technology.[2] These new types of sensors/actuators present an important potential for active vibration damping and health monitoring systems,[3] as well as for structural control devices.[4]

Three major processes have been developed to manufacture piezoelectric ceramic fibres: extrusion,[5] viscous suspension spinning process (VSSP),[6] and sol-gel processing.[7,8] These three manufacturing processes differ mainly in the nature of the precursor used and in the way the green fibres are formed prior to the firing and the sintering stages. In the extrusion process, the material is *pressed* with hydraulic presses through the nozzles of the extruder. In comparison, in spinning and sol-gel processes, the material is *pulled* through spinning nozzles. Processing conditions possibly induce large difference in the shape but also in the microstructure of the fibres (dimensional stability, preferred orientation, defects, etc...). This may have an important effect on the piezoelectric and mechanical properties of the resulting piezoelectric fibres.

Although some investigations[9–11] have been carried out to determine the piezoelectric performances of piezoelectric fibres, little has been published on their mechanical properties.[12] The aim of this study was to investigate the influence of the manufacturing process on the microstructure but also on the mechanical properties of different piezoelectric fibres. In order to achieve this goal, the microstructure of three commercially available piezoelectric fibres produced via three different manufacturing processes was observed with scanning electron microscopy and the mechanical properties of these fibres were determined with the single fibre test.

* Corresponding author. Tel.: +41-1-823-4486; fax: +41-1-821-6244.
E-mail address: xavier.kornmann@empa.ch (X. Kornmann).

0955-2219/03/$ - see front matter © 2003 Elsevier Ltd. All rights reserved.
doi:10.1016/S0955-2219(03)00364-9

2. Theory

2.1. Weibull analysis

The strength of brittle fibres is statistical in nature and the cumulative strength distribution function $P(\sigma)$ has the form of a Weibull distribution.[13] The probability of failure P_f of a fibre at a stress level equal to or less than the fracture strength σ_f can be described by the following function:

$$P_f(\sigma) = 1 - \exp\left[-\frac{V}{V_0}\cdot\left(\frac{\sigma-\sigma_u}{\sigma_0}\right)^{\beta}\right] \quad (1)$$

where V is the specimen volume, σ_u is a threshold stress below which the survival probability is 1, V_0 is a normalising constant, and σ_0 and β are, respectively, the scale and the shape parameters of the strength distribution. For fibres with a constant diameter, the Weibull expression can be rewritten in terms of the fibre length L and L_0 instead of V and V_0. Taking arbitrarily $\sigma_u = 0$ and $L_0 = 1$ leads to the following expression:

$$P_f(\sigma) = 1 - \exp\left[-L\cdot\left(\frac{\sigma}{\sigma_0}\right)^{\beta}\right] \quad (2)$$

The probability of fracture P_f can also be evaluated in a discrete manner as follows:

$$P_f = 1 - \frac{N_S + i}{N + i} \quad (3)$$

where N_s is the number of fibres surviving a given stress σ, N is the total number of fibres tested and i is a number between 0 and 1 (we took arbitrarily $i = 0.5$).

The scale and shape parameters σ_0 and β can then be obtained from a linear regression of the graph $\ln(-\ln(1-P_f))$ versus $\ln(\sigma)$ since:

$$\ln(-\ln(1 - P_f) = \ln L + \beta\cdot\ln(\sigma) - \beta\cdot\ln(\sigma_0) \quad (4)$$

The scale parameter σ_0 defines the overall stress level of the strength distribution, whereas the shape parameter β is inversely proportional to the width of the strength distribution. High scale and shape parameters describe the strength distribution of fibres with high strength and homogeneous structure, whereas low scale and shape parameters correspond to the strength distribution of poor quality fibres with the presence of large defects.

3. Experimental

3.1. Materials

Piezoelectric fibres based on lead zirconate titanate (PZT) were supplied by the three major commercial manufacturers in the world and will be denominated fibres A, B and C. All the fibres had an approximate diameter of 250 microns and were made of a similar material, namely PZT 5A. Fibres A were manufactured via an extrusion process[5] where the PZT powder mixed with a polymer binder under high shear conditions is extruded into green fibres that are subsequently fired and sintered at high temperatures. Fibres B were manufactured via a spinning process where the green fibres are spun from a mixture of PZT powder mixed with cellulose and a solvent and is then coagulated in a water bath. Fibres C were produced via the viscous–suspension–spinning process (VSSP),[14] where the precursor used to manufacture the green fibres is constituted of a mixture of PZT powder, deionised water, and viscose and is coagulated in a dilute sulphuric bath.

3.2. Microscopy

Scanning electron micrographs of the fracture surface of the three different piezoelectric fibres were taken with a Jeol field emission scanning electron microscope (FE 6300) with an acceleration voltage of 5 kV at low (250×) and high (1000×) magnification. The fracture surface of the fibres was coated with a 15 nm thick platinum layer by vapour deposition. An aluminium sample holder was especially constructed to hold the fibres in vertical position.

The diameter of each fibre at its fracture surface was measured under an optical microscope Zeiss Axioplan (Jena, Germany) with a magnification of 40. The measurements were performed with the software Image-Access. For the fibre whose diameter was not circular, the diameter measured was that of the smallest circle containing the fibre fracture surface.

3.3. Mechanical testing

The piezoelectric fibres were tested as received (i.e. unpoled state). They were first glued on a rectangular carton frame with an isocyanate glue. The frame was then clamped in a tensile machine and cut on both sides with scissors. The tested length of each fibre was 100 mm. Each fibre was preloaded with a force of 0.2 N with a speed of 0.4 mm/min. The test was then performed at a speed of 0.3 mm/min. For each type of piezoelectric fibres, 30 samples were tested following rigorously the same testing procedure. The tensile strength was calculated with the force at break divided by the area of the fracture surface. In each set of samples, about 50% of fibres broke near the grips. However, the Weibull analysis was performed with the data of all the tensile tests.

4. Results and discussion

4.1. Scanning electron microscopy

The fracture surfaces of each type of piezoelectric fibres were observed at low magnification (250×) with a

scanning electron microscope. The micrographs presented in Fig. 1 indicate that the three fibres show large differences in the morphology of their fracture surface even though all the fibres broke in a brittle manner. Fibres A present systematically an imperfection constituted of a flattened area indicated by an arrow in Fig. 1a. This defect may be linked to the manufacturing process. One explanation could be that after the extrusion, the green fibres were placed on a flat surface prior or during the firing and the sintering steps. The fibres may have been subjected to creep under own weight, which would explain the presence of the flattened area. The cross-section of fibres B is almost perfectly circular (see Fig. 1b). Interestingly, it is possible to see crystals (see arrow in Fig. 1b), which have grown on the surface of the fibre. Fibres C present the most irregular cross-section (see Fig. 1c). The cross-section of the fibre is oval and not circular and large porosities (ca. 20% of the total surface area) can be observed on the fracture surface of the fibre. These large defects, observed with almost all the fibres of this type, are probably linked to the manufacturing process (i.e. VSSP). Indeed, French et al.[14] inventors of the VSSP mention in one of their publication that trapped air in the spin mix must be removed under vacuum, as air in the spin mix will cause hollow filaments. This problem has apparently still not completely been solved in the commercial process.

The magnification of the scanning electron microscope was then increased to 1000 in order to observe the microstructure of the fibres (see Fig. 2). It appears that the microstructure of fibres A (Fig. 2a) is significantly finer than that of fibres B and C (Fig. 2b and c). This difference was also observed by Nelson et al.[15] This is apparently linked to the manufacturing process since fibres A are produced via extrusion process whereas fibres B and C are manufactured via spinning processes. Microscopic pores are observed in all the samples but these pores are finer in fibres A.

The microstructure of the piezoelectric fibres but also the presence of macrostructural defects has a direct influence on the mechanical properties of the piezoelectric fibres, as we will see in the next section.

4.2. Tensile properties

Table 1 presents the average diameters and the Young's moduli of the different fibres with their respective standard deviation. The main diameter of all the three fibres is greater than 250 μm. This illustrates the fact that it is difficult to control precisely the diameter of the piezoelectric fibres during their manufacturing process. Fibres C present a large standard deviation of their fibre diameter (±13 μm) in comparison with the two other types of fibres. This illustrates the irregularity in the cross-section of these fibres and may be linked to the manufacturing process. It is however interesting to notice that fibres B that are also manufactured via a spinning process are much more uniform than the fibres C. Apparently, extrusion seems to be the most suitable process to produce fibres with a uniform diameter. The *E*-modulus of the piezoelectric fibres is around 40 GPa. This value is lower than the typical modulus of PZT, which is around 50 GPa. Part of this difference is possibly due to the microscopic porosity observed in the three piezoelectric fibres. The processes used to manufacture piezoelectric fibres generate apparently more microscopic porosity than conventional piezoceramic manufacturing processes. Interestingly, fibres C, which present in many cases large porosities, present also the lowest *E*-modulus. This means that these porosities may have a detrimental effect on the electromechanical performances of these fibres.

Fig. 3 presents the typical stress–strain behaviour of the three piezoelectric fibres (each curve corresponds to the tensile test of one fibre, representative of the tensile behaviour of each fibre type). It is interesting to see that the three piezoelectric ceramic fibres present a large non-linear behaviour. This non-linearity cannot find its origin in an eventual slippage of the fibres at the grips of the tensile machine according to the fact that measurements performed with an optical method lead to similar results. This non-linearity is a peculiar behaviour for ceramic materials. This effect is apparently linked to the piezoelectric nature of the fibres. Indeed, it is likely that deformations of the fibres induce an orientation of the dipoles present in the piezoelectric material since the

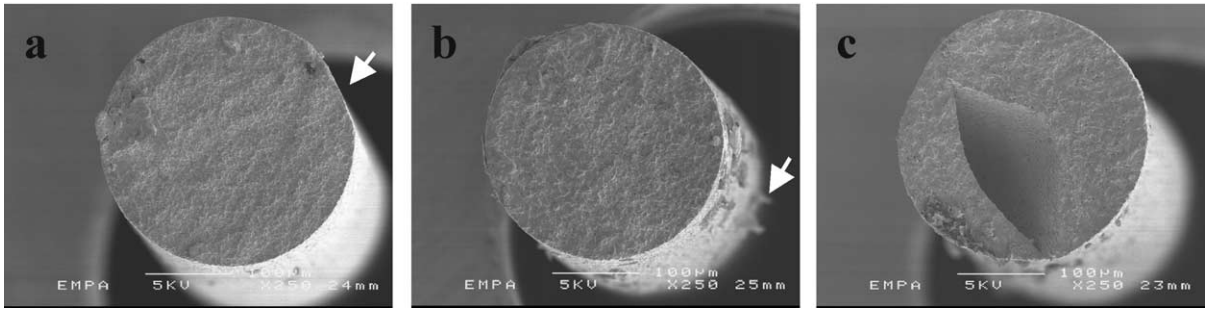

Fig. 1. Scanning electron micrographs of the fracture surfaces of fibres A (a), B (b), and C (c).

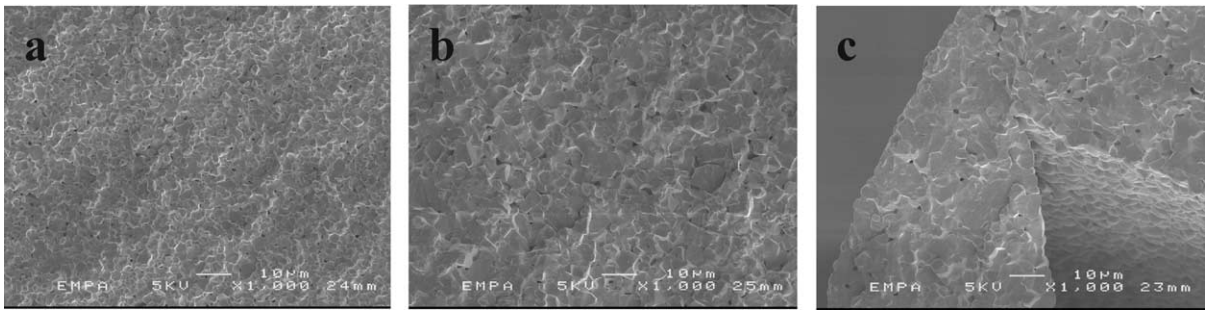

Fig. 2. Scanning electron migrographs of the microstructure of fibres A (a), B (b), and C (c).

Table 1
Diameter and *E*-modulus of fibres A, B, and C

	Fibres A	Fibres B	Fibres C
Diameter (μm)	268±2.5	264±5	266±13
E-Modulus (GPa)	38.5±1.1	40±1.7	37.7±4.5

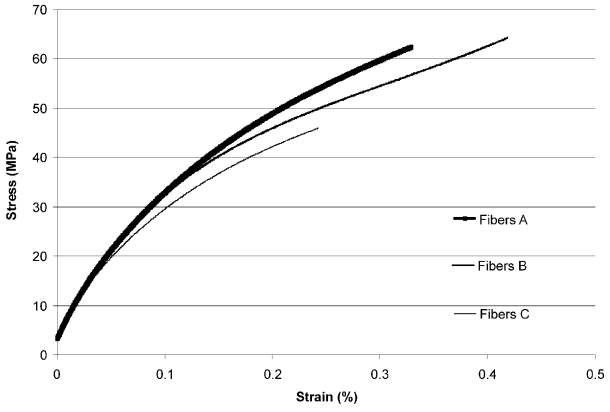

Fig. 3. Typical stress–strain behaviour of fibres A, B, and C.

fibres tested were in an unpoled state. If one look at the typical stress–strain behaviour of fibres B it is possible to distinguish a change of slope above a strain of 0.3%. This effect may be due to the fact that at this level of strain, most of the dipoles present in the material are already oriented so that this generates a modulus increase. This effect is not observed with the two other fibres because they break before this phenomenon can occur. Further tests are required to explain more into details the stress–strain behaviour of these fibres. Fig. 3 shows also that the tensile strength of the three types of fibres is also significantly different. A Weibull analysis was performed in order to characterise the strength distribution of the piezoelectric fibres.

4.3. Strength distribution analysis

Fig. 4 presents the probability of failure of each type of fibres as a function of applied stress. The closed symbols correspond to cases where the fibres broke near the grips. These data were not disregarded for the

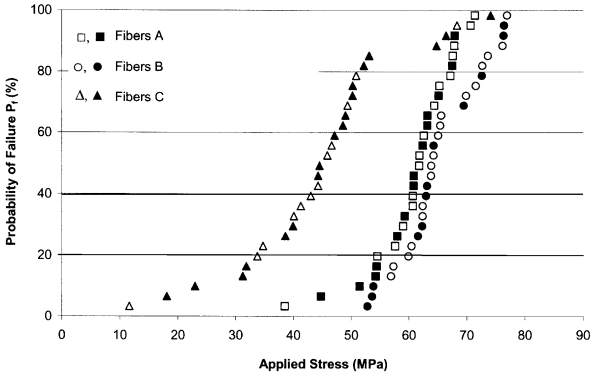

Fig. 4. Weibull plots of fibres A (□, ■), B (○, ●), and C (△, ▲). The closed symbols indicate cases where the fibres broke near the grips. The fibre length is 100 mm.

Weibull analysis according to the fact that they do not change fundamentally the shape of the strength distribution of each fibre. From these diagrams, commonly called Weibull plots, it can be clearly seen that fibres C break at significantly lower stress than the two other fibres. Moreover, the strength distribution of these particular fibres is much broader.

In order to perform a finer analysis of these data, the scale and shape parameters, σ_0 and β (i.e. Weibull parameters) were determined according to the method described in the theoretical section and are presented in Table 2. By definition, the scale parameter σ_0 defines the overall stress level of the strength distribution, whereas the shape parameter β is inversely proportional to the width of the strength distribution. The strength distribution of high quality fibres corresponds therefore to high scale and shape parameters.

The strength distribution of fibres C has a significantly lower scale parameter than the ones for the two other fibres. This difference can be very well correlated with the microscopical observations of the fibres. Indeed, the scanning electron micrographs have indicated the presence of large porosities in fibres C. These large defects lower therefore significantly the strength of the fibres. Actually, even the presence of a small defect in fibres A (flattened area) seems to have a damaging effect on the resulting strength of the fibres since the

Table 2
Weibull parameters of fibres A, B, and C

	Fibres A	Fibres B	Fibres C
Scale parameter σ_0 (MPa)	63.8	68	49.5
Shape parameter β	11.7	9.6	3.9

scale parameter of their strength distribution is lower than that of fibres B. The analysis of the different shape parameters reveals that fibres C, with the lowest shape parameter (3.9), present the most spread strength distribution due to the presence of defects of different sizes in the fibres. Interestingly, fibres A, which show the finest microstructure in comparison with the two other fibres, present the highest shape parameter (11.7).

The overall conclusion of this Weibull analysis is that both the spinning process (fibres B), if well controlled, and the extrusion process (fibres A) are suitable to manufacture high quality piezoelectric fibres.

5. Conclusions

Piezoelectric ceramic fibres manufactured via different manufacturing processes (extrusion, spinning) present large differences in terms of microstructure and mechanical properties. Microscopical observations indicate that the (VSSP) generates inhomogeneous fibres (Fibres C) with large porosities, whereas the extrusion process gives apparently the possibility to manufacture more homogeneous fibres (Fibres A) with finer microstructure. In contrast with the fibres manufactured via the VSSP, the third type of fibres (Fibres B), manufactured also via a spinning process presents a more homogeneous structure with low amount of defects, indicating that both extrusion and well controlled spinning processes offer the possibility to manufacture high quality fibres. Interestingly, the differences observed microscopically between the fibres are well correlated with their strength distribution analysis (i.e. Weibull analysis). Thus, the strength distribution of fibres C presents low scale and shape parameters due to the present of large defects, whereas those of fibres A and B with a more homogeneous structure show high scale and shape parameters. Finally, all the fibres present a non-linear stress–strain behaviour, which is apparently linked to their piezoelectric nature. Further investigations are required to confirm this hypothesis.

Acknowledgements

Mr. R. Bächtold from the High Performance Ceramics Department at EMPA is acknowledged for the mechanical testing of the single fibres. The authors thank also Mrs. E. Strub from the Wood Department at EMPA for the electron microscopy work.

References

1. Safari, A. and Janas, V. F., Processing of fine-scale piezoelectric ceramic/polymer composites for transducer applications. *Ferroelectrics*, 1997, **196**, 187–190.
2. Bent, A. A. and Hagood, N. W., Piezoelectric fibre composites with interdigitated electrodes. *J. Int. Mat. Syst. Struct.*, 1997, **8**, 903–919.
3. Schultz, M. J., Sundaresan, M. J. and Ghoshal, A., Active fibre composites for structural health monitoring. *SPIE Conf. Proc.*, 2000, **3992**, 13–24.
4. Bent, A. A., Active fibre composite material systems for structural control applications. *SPIE Conf. Proc.*, 1999, **3674**, 166–177.
5. Strock, H. B., Pascucci, M. R., Parish, M. V., Bent, A. A. and Shrout, T. R., Active PZT fibres, a commercial production process. *SPIE Conf. Proc.*, 1999, **3675**, 22–31.
6. Cass, R. B., Fabrication of continuous ceramic fibre by the viscous suspension spinning process. *Cer. Bull.*, 1991, **70**, 424–429.
7. Glaubitt, W., Sporn, D. and Jahn, R., Sol-gel processing of PZT long fibres. *8th CIMTEC Conf. Proc.*, 1995, **10**, 47–54.
8. Selvaraj, U., Prasadarao, A. V., Komarneni, S., Brooks, K. and Kurtz, S., Sol-gel processing of $PbTiO_3$ and $Pb(Zr_{0.52}Ti_{0.48})O_3$ fibres. *J. Mater. Res.*, 1992, **7**, 992–996.
9. Yoshikawa, S., Selvarj, U., Moses, P., Witham, J., Meyer, R. and Shrout, T., $Pb(Zr,Ti)O_3$ [PZT] fibres—fabrication and measurement methods. *J. Int. Mat. Syst. Struct.*, 1995, **6**, 152–158.
10. Bystricky, P., Ceramic piezoelectric fibres: correlating single fibre properties with active fibre composite performance. *SPIE Conf. Proc.*, 2000, **3895**, 552–559.
11. Steinhausen, R., Hauke, T., Beige, H., Watzka, W., Lange, U., Sporn, D., Gebhardt, S. and Schönecker, A., Properties of fine scale piezoelectric PZT fibres with different Zr content. *J. Eur. Ceram. Soc.*, 2001, **21**, 1459–1462.
12. Yoshikawa, S., Selvaraj, U., Moses, P., Jiang, Q. and Shrout, T., $Pb(Zr,Ti)O_3$ [PZT] fibres—fabrication and properties. *Ferroelectrics*, 1994, **154**, 325–330.
13. Weibull, W., A statistical distribution function of wide applicability. *J. Appl. Mech.*, 1951, **18**, 1426–1430.
14. French, J. D., Weitz, G. E., Luke, J. E., Cass, R. B., Jadidian, B., Bhargava, P. and Safari, A., Production of continuous piezoelectric ceramic fibres for smart materials and active control devices. *SPIE Conf. Proc.*, 1997, **3044**, 406–4012.
15. Nelson, L. J. and Bowen, C. R., Determination of the piezoelectric properties of fine scale PZT fibres. *Key Eng. Mat.*, 2002, **206–213**, 1509–1512.